



Supporting Information

© Copyright Wiley-VCH Verlag GmbH & Co. KGaA, 69451 Weinheim, 2019

Fatty Acid Binding to Human Serum Albumin in Blood Serum Characterized by EPR Spectroscopy

Haleh H. Haeri, Bettina Schunk, Jörg Tomaszewski, Heike Schimm, Marcos J. Gelos, and Dariush Hinderberger* © 2019 The Authors. Published by Wiley-VCH Verlag GmbH & Co. KGaA. This is an open access article under the terms of the Creative Commons Attribution Non-Commercial NoDerivs License, which permits use and distribution in any medium, provided the original work is properly cited, the use is non-commercial and no modifications or adaptations are made.

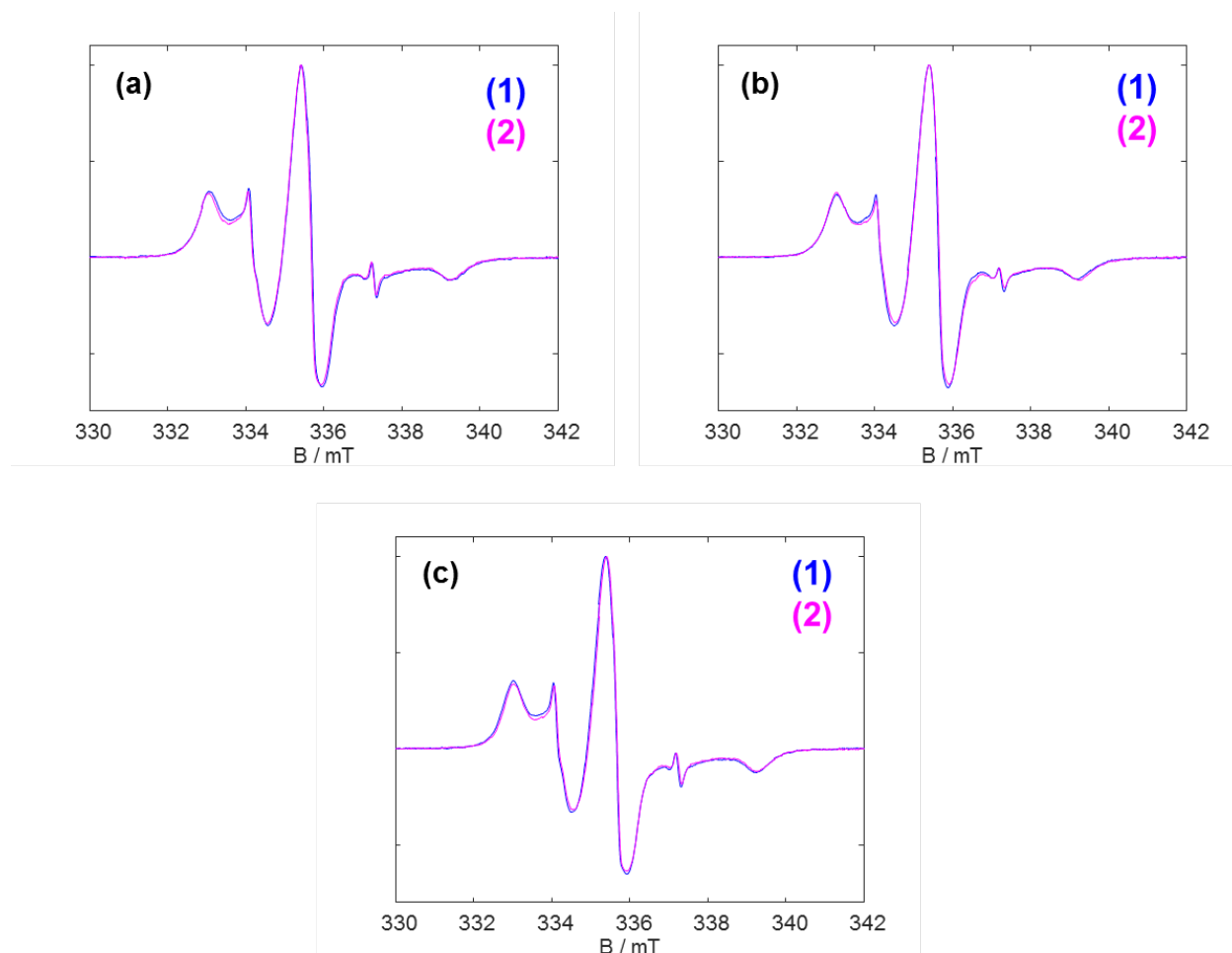


Fig.S1. Stability of the samples and therefore reproducibility of results were examined for three samples of control group (numbered as 17(a), 18 (b) and 19 (c)) at their 1:4 loading ratio. The spectra indicated as (1 in blue), are the first time measured ones and the ones with (2 in magenta) are those which are measured after a three months' time, kept in -80°C conditions. As can be seen the spectra fully overlay each other and results are reproducible.

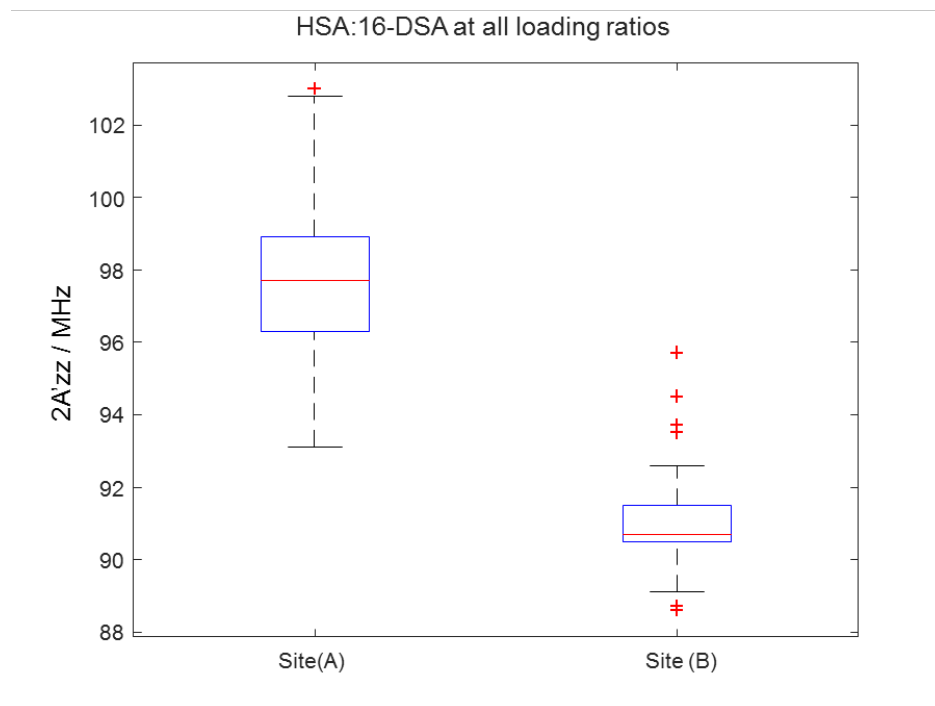


Fig.S2. Boxplot of hyperfine couplings for all loading ratios of HSA: 16-DSA in terms of their binding affinities, sites (A) and (B). The medians are shown by red lines. The high affinity binding sites (A) have larger couplings which reflect the effect of (negatively) charged ions and different orientations of the spin probe molecule, 16-DSA.

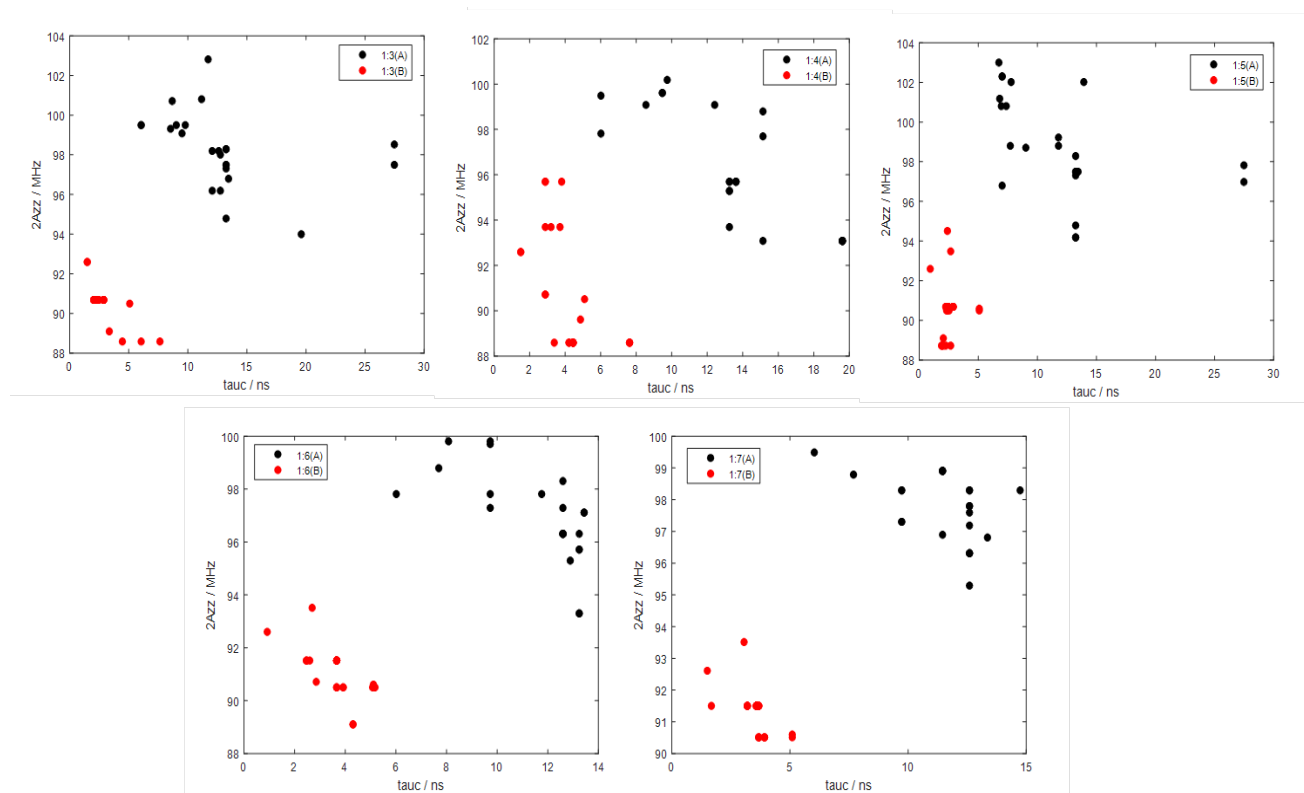


Fig.S3. Correlation between hyperfine coupling and rotational correlation times at different loading ratios. There is no strong correlation between these variables, so they could be considered as independent variables. However, one observes a distinct separation between related data sets of two binding classes (A) and (B).

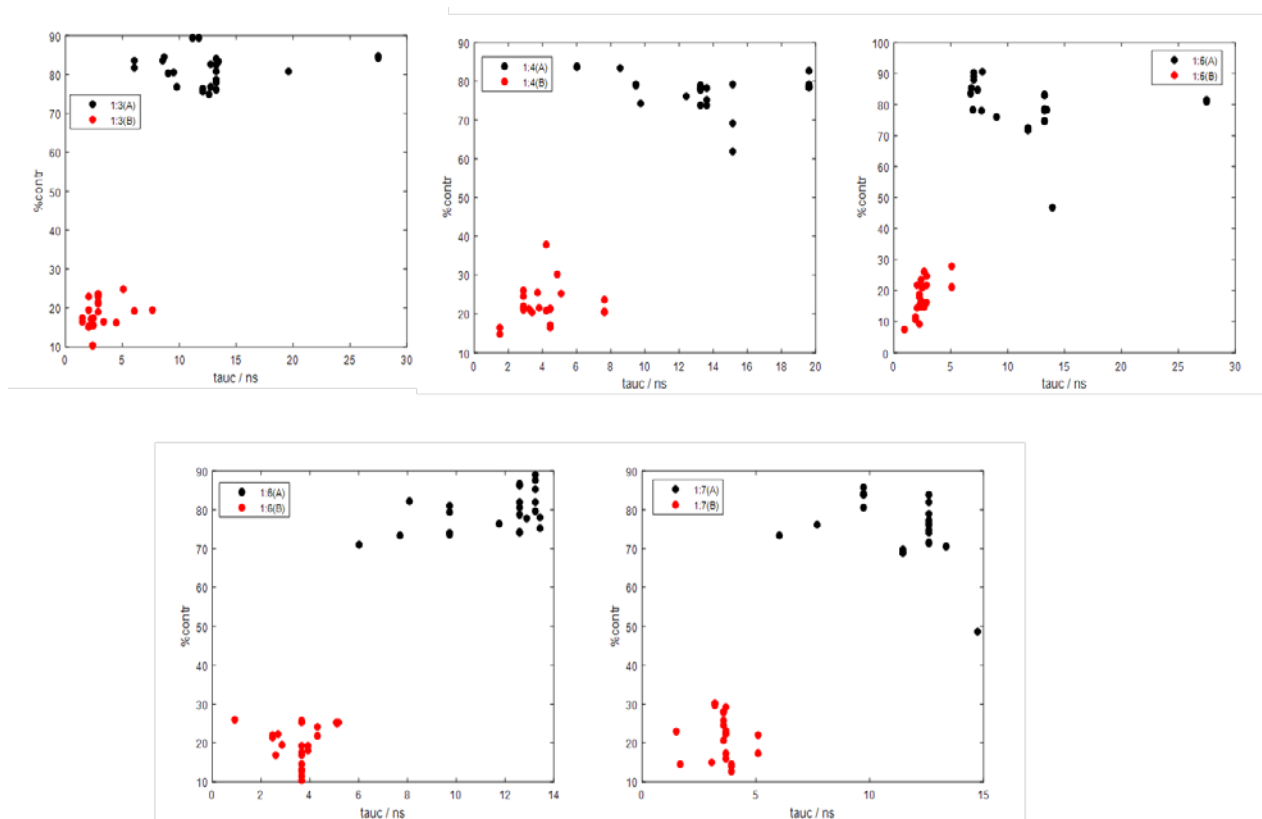


Fig.S4. Correlation between population (contribution) of each class of binding sites (A) and (B) and correlation times at different loading ratios. The variable space of correlation times has smaller spread compared to the population variable. Two separated different motional regimes are apparent and can be distinguished based on their rotational correlation times.

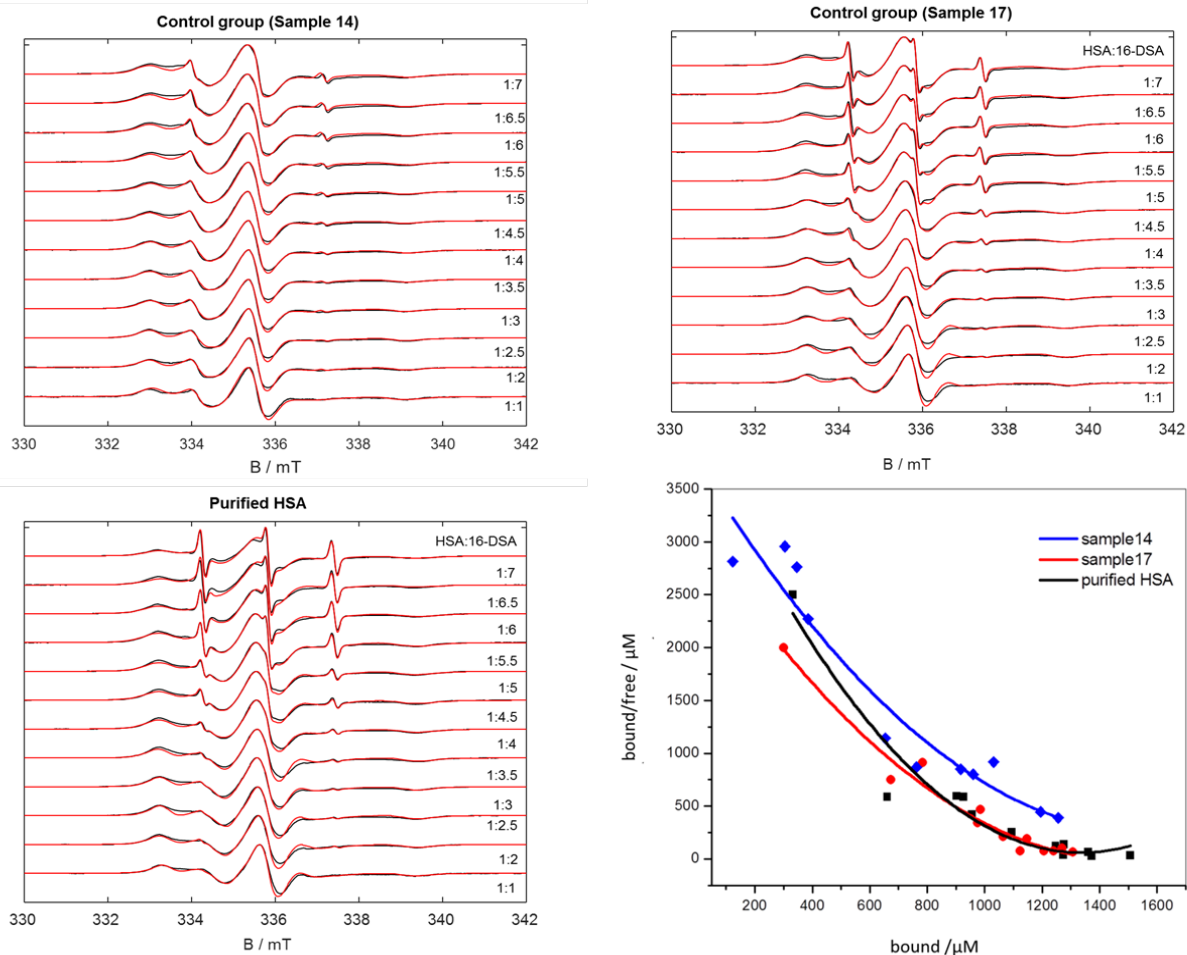


Fig.S5. Experimental (in black) and simulated (in red) spectra for two samples of control group in comparison with the purified HAS are given. The lower right panel depicts the Scatchard plots of these three samples. Bound and non bound fractions of FAs are obtained by simulations and were plotted according to Scatchard equation (eq.1)

$$\frac{B}{F} = -\frac{1}{k_D}(B - B_0) \text{ (eq. 1)}$$

In which “*B*” is the bound and “*F*” is the free fraction of FAs. The *k_D* Indicates the dissociation constant and “*B₀*” is the zero intercept at *B*/*F*=0.

The downward plots show negative cooperativity and slight deviations from linearity for all three cases. As can be seen from spectra, sample number 17 behaves rather similar to the purified HSA, although still has less free component. Sample numbered as 14 shows much less free component contributions compared to two other samples. For example, its value is about tenth of the corresponding value of purified HSA at a loading ratio of 1:7. This sample could be considered among the ones who have nonspecific binding sites.